Electronic Supplementary Material (ESI) for RSC Advances.
This journal is © The Royal Society of Chemistry 2020

Electronic Supporting Information

Thermodynamically Stable Vesicle Formation of Biodegradable Double mPEG-Tailed Amphiphiles with Sulfonate Head Group

Rita Ghosh[a§], Joykrishna Dey[a]* and B. V. N. Phani Kumar[b]

[a]Department of Chemistry, Indian Institute of Technology Kharagpur, Kharagpur-721302, India

§Current address: Department of Chemistry, St. Joseph's College Autonomous, Bangalore-560027, India

[b]NMR, **CATERS**, CSIR−Central Leather Research Institute, Adyar, Chennai−600020, India.

1. Synthesis

The amphiphiles were synthesized by the Michael addition reaction of sodium-2,3-dimercaptopropanesulfonate with poly(ethylene glycol) methyl ether methacrylate by thiol−ene "click" chemistry (**Scheme S1**) following reported method.[1-3] In brief, sodium-2,3-dimercaptopropanesulfonate (1 eq) was reacted with mPEG (2.2 eq) in methanol at room temperature for 12 h in the presence of TEA (2.2 eq). The solvent was then evaporated and the product was obtained as viscous liquid for $(mPEG_4)_2SO_3Na$ and as white, hygroscopic solid for $(mPEG_{23})_2SO_3Na$. The unreacted materials were removed by washing the product repeatedly with *n*-hexane. Then the pure product was air dried under vacuum. Chemical structures of $(mPEG_4)_2SO_3Na$ and $(mPEG_{23})_2SO_3Na$ were identified by the ^1H- and ^{13}C-NMR spectra. The representative ^1H- and ^{13}C-NMR spectra of $(mPEG_4)_2SO_3Na$ have been depicted in **Figure S1** and **S2**, respectively.

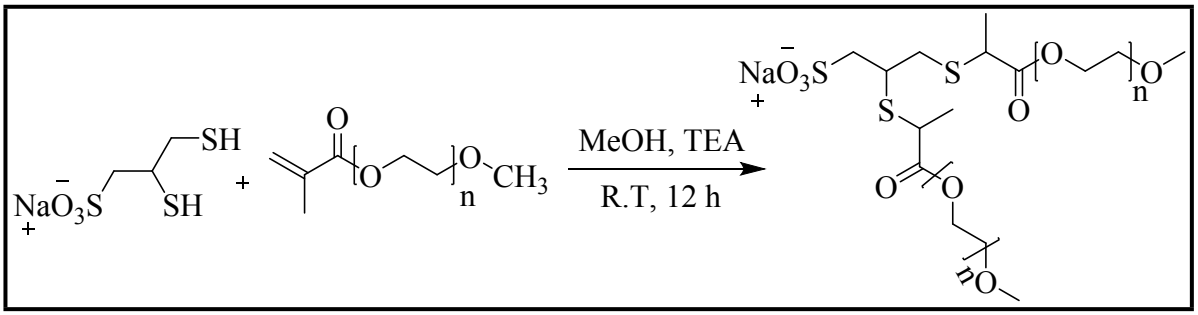

Scheme S1 Reaction scheme for the synthesis of $(mPEG_4)_2SO_3Na$ and $(mPEG_{23})_2SO_3Na$.

2. Chemical identification data of $(mPEG_4)_2SO_3Na$ and $(mPEG_{23})_2SO_3Na$

MW: 828.30g ($(mPEG_4)_2SO_3Na$) and 2428.3 ($(mPEG_{23})_2SO_3Na$), **State:** colorless semi solid ($(mPEG_4)_2SO_3Na$) and white hygroscopic solid ($(mPEG_{23})_2SO_3Na$), **Yield:** ~ 80%, **FTIR (KBr, cm^{-1}):** absence of double bond is confirmed by absence of C-H stretching at 3000 cm^{-1} and no band at 2565 cm^{-1} confirms absence of S-H stretching. Peak at 1738 cm^{-1} shows presence of C=O stretching of ester group and peak at 638 cm^{-1} shows presence of C-S stretching. **^{1}H-NMR (D_2O, 600 MHz):** δ (ppm) 1.254 ($COCH\boldsymbol{CH_3}$, t, 3H), 2.885 ($SO_3NaCH\boldsymbol{CH_2}$, d, 2H), 2.895 ($S\boldsymbol{CH_2}$-CH, d, 2H), 3.002 ($SCH_2\boldsymbol{CH}CO$, m, 1H), 3.358 ($O\boldsymbol{CH_3}$, s, 3H), 3.551 ($CO\text{-}OCH_2\boldsymbol{CH_2}$, t, 2H), 3.663 (long chain glycolic $C\boldsymbol{H_2}$, m, 36H for DPEGS1 and 208H for DPEGS2), 3.729 ($SO_3Na\ \boldsymbol{CH_2}$, t, 2H), 4.351 ($CO\text{-}O\boldsymbol{CH_2}\text{-}CH_2$, dd, 2H). **^{13}C-NMR (D_2O, 600 MHz):** δ (ppm) 178.5 ($\boldsymbol{C}OOCH_2$), 64.7, 69.5, 70.5, 70.9, 73.6 (ether $\boldsymbol{C}H_2$), 58.4 ($O\boldsymbol{C}H_3$), 51.4 ($S\boldsymbol{C}H_2CH$), 40.2 ($SCH_2\boldsymbol{C}H$), 34.8 ($S\boldsymbol{C}H_2\ CH_2COOH$), 26.4 ($SCH_2\ \boldsymbol{C}H_2COOH$), 16.4 ($\boldsymbol{C}H_3$).

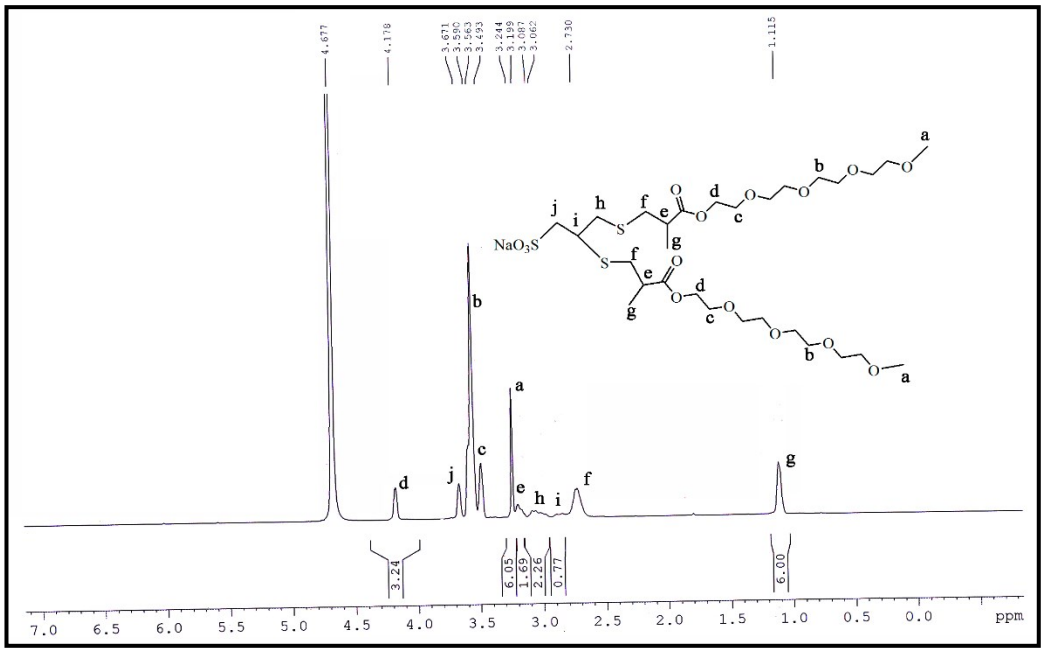

Figure S1 ^{1}H-NMR spectrum of $(mPEG_4)_2SO_3Na$ in D_2O solvent.

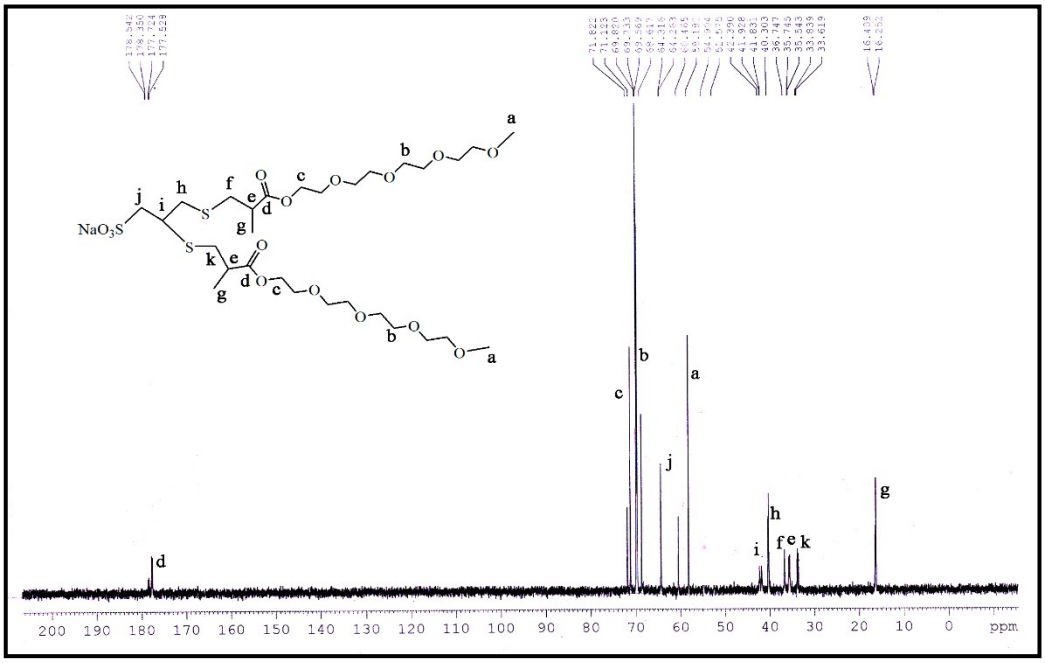

Figure S2 ^{13}C-NMR spectrum of $(mPEG_4)_2SO_3Na$ in D_2O solvent.

3. Experimental methods

3.1. Nuclear magnetic resonance (NMR) spectra

The ^{1}H NMR measurements were performed using Bruker (AVANCE-III) and JEOL (ECA-500) operating at 400 MHz and 500 MHz FT-NMR spectrometers, respectively. The variable-temperature ^{1}H chemical shifts, spin-lattice relaxation times (T_1), spin-spin relaxation times (T_2) were determined for $(mPEG_4)_2SO_3Na$ and $(mPEG_{23})_2SO_3Na$ in D_2O (1 mM). The ^{1}H T_1 and T_2 measurements were made by employing inversion recovery and CPMG pulse sequences, respectively.[4] The observed magnetization recovery data (both T_1 and T_2) exhibited a single-exponential decay and corresponding data were analyzed with the aid of three and two-parameter fits, respectively. The estimated errors in both T_1 and T_2 data were about 2%. While, translational self-diffusion coefficients (D) were made for $(mPEG_4)_2SO_3Na$ and $(mPEG_{23})_2SO_3Na$ at 25 ^{o}C alone. For ^{1}H translational self-diffusion measurements, bipolar pulse pair longitudinal encode-decode (BPPLED) sequence was utilized.[5] The experimental and processing details were as described elsewhere.[6] The diffusion coefficients were obtained by fitting the experimental data to the Stejskal-Tanner equation:[7]

$$I = I_o e^{-kD} \qquad (1)$$

where I_0 is the peak intensity in the absence of gradient pulses, the parameter $k = (\gamma_n \delta g)^2 (\Delta - \delta/3)$, γ_n is the magnetogyric ratio, g is the gradient amplitude, while δ and Δ represent gradient duration and diffusion time, respectively, and D is the translational self-diffusion coefficient.[7] The estimated error in D was < 2%. For brevity, only three representative ^{1}H resonances *a* (OCH_3; singlet at 3.290 ppm), *b* (OCH_2; triplet at 3.607, and 3.614 ppm) and *g* ($CH(CH_3)$); doublet (1.149, 1.161 ppm)) of $(mPEG_4)_2SO_3Na$ and $(mPEG_{23})_2SO_3Na$ (see **Figure S1**) were used in spin-relaxation analysis, whereas *b* (OCH_2)

protons were utilized in the self-diffusion measurements. Self-diffusion coefficient (D) values were used to calculate the hydrodynamic radii (R_h) with the aid of Stokes-Einstein equation:

$$R_h = k_B T/6\pi\eta D \quad (2)$$

where the symbols have their usual meaning, provides the size of morphologies encountered by the surfactant systems. The value of η of D_2O was taken as 1.098 mPa s at 25 ^oC.

3.2. Surface tension measurements

Surface tension (γ/mNm^{-1}) measurements were carried out using a Du Nuöy ring surface tensiometer (model 3S, GBX, France) fitted with a thermostating beaker holder. The instrument was calibrated by measuring the γ value of Milli Q water (pH 6.7, resistivity 18 MΩ cm). The platinum-iridium ring was washed with EtOH–HCl solution (50:50 v/v) and was burnt in the oxidizing flame immediately before use. The stock solutions of $(mPEG_4)_2SO_3Na$ and $(mPEG_{23})_2SO_3Na$ were prepared in pH 7.0 phosphate buffer (20 mM). For every measurement, an aliquot of the stock solution was poured into a known volume of buffer in a Teflon beaker and kept for equilibration for 10 min at 25 ^oC. The temperature was controlled by JULABO MC water-circulating bath with a temperature accuracy of ±0.1 ^oC. For each surfactant concentration, the γ value was measured thrice and an average value was noted.

3.3. Steady-state fluorescence measurements

The steady-state fluorescence spectra of the fluorescent probes (NPN and DPH) were measured on a PerkinElmer LS-55 luminescence spectrometer equipped with a temperature-controlled cell holder. A SPEX Fluorolog-3 (FL3-11, USA) spectrophotometer was used to record fluorescence emission spectra of Py. Aliquots of stock solutions of Py or DPH (0.1 mM in MeOH) and $(mPEG_4)_2SO_3Na$ or $(mPEG_{23})_2SO_3Na$ (in pH 7.0 buffer) were diluted in a 5 mL volumetric flask by buffer solution. The emission spectra of the solutions containing Py were

recorded in the wavelength range of 350–550 nm at an excitation wavelength (λ_{ex}) of 340 nm using excitation and emission slit widths of 5 and 1 nm, respectively. The λ_{ex} for solutions containing DPH was 350 nm and the emission spectra were recorded in the wavelength range of 360–550 nm.

3.4. Fluorescence anisotropy measurements

An LS-55 luminescence spectrometer (Perkin Elmer, UK) equipped with a magnetically stirred cuvette holder and a polarization accessory that uses the L-format instrumental configuration was used to measure steady-state fluorescence anisotropy of DPH probe. The anisotropy was calculated using the equation: [8]

$$r = (I_{VV} - GI_{VH}) / (I_{VV} + 2GI_{VH}) \quad (3)$$

where I_{VV} and I_{VH} are the fluorescence intensities when the emission polarizer is oriented parallel and perpendicular to the excitation polarizer, and G (= I_{HV}/I_{HH}) is the instrumental grating factor. The G factor and *r* values were automatically determined by the software supplied by the manufacturer. In all measurements, the *r* value was recorded over an integration time of 10 s, and an average of six readings was noted as the *r* value. The samples were excited at λ_{ex} = 350 nm and the anisotropy of emission was measured at 450 nm using excitation and emission slit widths of 2.5 nm and 2.5−10.0 nm, respectively. A 430 nm emission cut-off filter was placed between the excitation and emission monochromators to eliminate the effect of scattered and stray radiation. All solutions were equilibrated at the desired temperature for at least 10 min before measurement. Temperature was controlled by use of Thermo Neslab RTE-7 circulating bath.

3.5. Time-resolved fluorescence measurements

The time-resolved fluorescence experiments were performed on an Optical Building Blocks Corporation Easylife instrument equipped with a nanosecond diode laser (λ_o = 380 nm). The fluorescence decay kinetics of DPH were monitored at λ_{max} = 450 nm. The decay curves were analysed by single exponential or bi-exponential iterative fitting program. The randomness of residual plot and χ^2 value (0.8−1.2) were used to determine best fit. The micrviscosity (η_m) value was calculated from the measured fluorescence lifetime (τ_f) and *r* values using Debye−Stokes−Einstein relation:[9]

$$\eta_m = k_B T \tau_R / v_h \quad (4)$$

where v_h is the hydrodynamic volume (313 Å^3) [10] of the DPH probe. The rotational correlation time, τ_R, was calculated using Perrin's equation:[9]

$$\tau_R = \tau_f (r_o / r - 1)^{-1} \quad (5)$$

where r_o (= 0.362) [11] is the steady-state fluorescence anisotropy of DPH in a highly viscous solvent.

3.6. Isothermal titration calorimetry (ITC)

Thermometric parameters were measured with a microcalorimeter (Microcal iTC_{200}, U.S.A). In a microsyringe of capacity 40 μL, solution of $(mPEG_4)_2SO_3Na$ (20 mM) or $(mPEG_{23})_2SO_3Na$ (10 mM) was taken and added in multiple stages to a known volume of pH 7.0 buffer kept in the calorimeter cell of capacity 200 μL under constant stirring conditions. The stirring speed was fixed at 400 rpm and Milli-Q water was taken at reference cell. The thermograms for the stepwise heats of dilution were recorded for both amphiphiles. Enthalpy calculations were performed with the help of ITC software. All measurements were carried out at 25 ^oC. The $\Delta_m H^o$ value was obtained by taking one half of the difference between the initial

enthalpy and the final enthalpy corresponding to plateau in each plot of **Figure S7**. The $\Delta_m G^o$ value was calculated from the measured *cac* value using the relationship:[12]

$$\Delta_m G^o = (1 + \beta)\, RT\, ln(cac) \quad (6)$$

where β is the degree of counterion binding of the surfactant molecule which is usually taken as 0.8 for anionic surfactants [13] and *cac* is the critical aggregation concentration of the amphiphile. The $\Delta_m S^o$ value was evaluated by the Gibbs equation:

$$\Delta_m S^o = (\Delta_m H^o - \Delta_m G^o)/ T \quad (7)$$

3.7. Dynamic light scattering

The measurements of hydrodynamic size and size distribution histograms were carried out with a Zetasizer Nano ZS (Malvern Instrument Lab, Malvern, U.K.) dynamic light scattering (DLS) spectrometer that uses a He−Ne laser operated at 4 mW at λ_o = 632.8 nm as the light source. All scattering photons were collected at a 173^o scattering angle (back scattering). The solutions for DLS measurements were filtered through a 0.22 μm filter paper (Millipore Millex syringe filter) at least twice in to a 1 cm^2 glass cuvette. The sample was equilibrated inside the DLS optical system chamber at 25 ^{o}C for 10 min before the measurement. The data acquisition was done for at least 100 counts, and each experiment was repeated three times. The value of diffusion constant (D) was calculated using cumulant analysis and the corresponding R_h value was obtained from equation (2). The surface zeta (ζ)-potential of the aggregates was determined using the same DLS spectrometer. An average of the values of three successive measurements was taken for each sample.

3.8. Transmission electron microscopy (TEM)

Transmission electron micrographs of surfactant solutions at different concentrations (> *cmc*) were measured at room temperature on an HRTEM (JEOL-JEM 2100, Japan) operating at an

accelerating voltage of 200 kV. For every sample, 4 µL of surfactant solution was placed on to a carbon-coated copper grid (400 mesh size) and after 1 min the excess water was blotted off by use of a filter paper. The specimen thus prepared were placed in vacuum desiccators overnight for drying until before measurement. Each measurement was repeated at least thrice to check the reproducibility.

3.10. Atomic force microscopy (AFM)

For AFM measurements, a Nanoscope IIIA from Digital Instruments in tapping mode under ambient conditions was employed. One drop of 2 mM $(mPEG_4)_2SO_3Na$ or $(mPEG_{23})_2SO_3Na$) solution was placed on a clean mica surface and the specimen was left overnight in a vacuum desiccators.

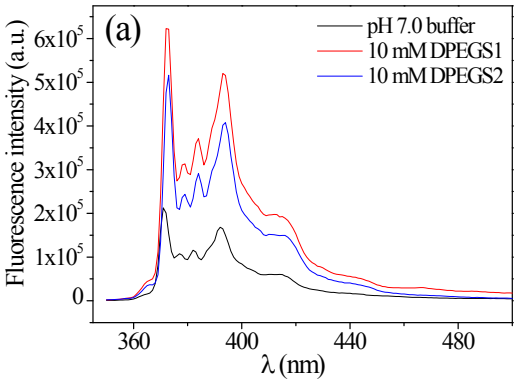

Figures S3 Fluorescence spectra of pyrene in buffer in the absence and presence of $(mPEG_4)_2SO_3Na$ and $(mPEG_{23})_2SO_3Na$.

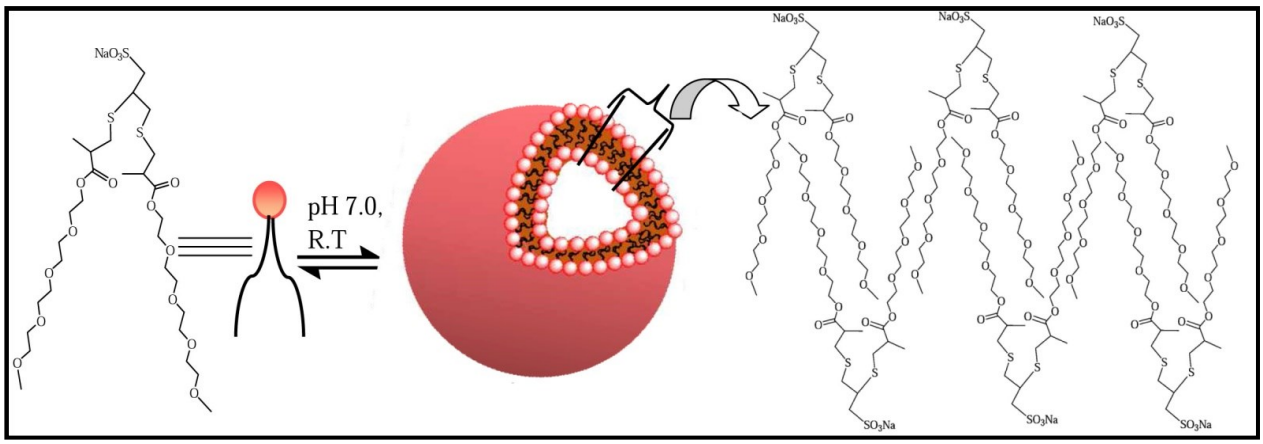

Figure S4 Schematic representation of bilayer vesicle formation by the $(mPEG_4)_2SO_3Na$ molecules.

Table S1 The steady-state fluorescence anisotropy (r) and lifetime (τ_f) of DPH probe, and microviscosity (η_m) values of the vesicles in solutions of different concentrations of $(mPEG_4)_2SO_3Na$ and $(mPEG_{23})_2SO_3Na$ at 25 °C.

Surfactant	C_s (mM)	r (± 0.001)	τ_f (ns) (± 0.01)	η_m (mPa s) (± 1.0)
$(mPEG_4)_2SO_3Na$	1.0	0.152	4.84	46.0
	2.0	0.153	4.91	47.0
	3.0	0.158	4.95	50.0
	4.0	0.162	4.99	53.0
	5.0	0.165	5.06	56.0
$(mPEG_{23})_2SO_3Na$	1.0	0.130	4.63	34.0
	2.0	0.131	4.67	35.0
	3.0	0.132	4.70	36.0
	4.0	0.133	4.72	36.0
	5.0	0.135	4.79	37.0

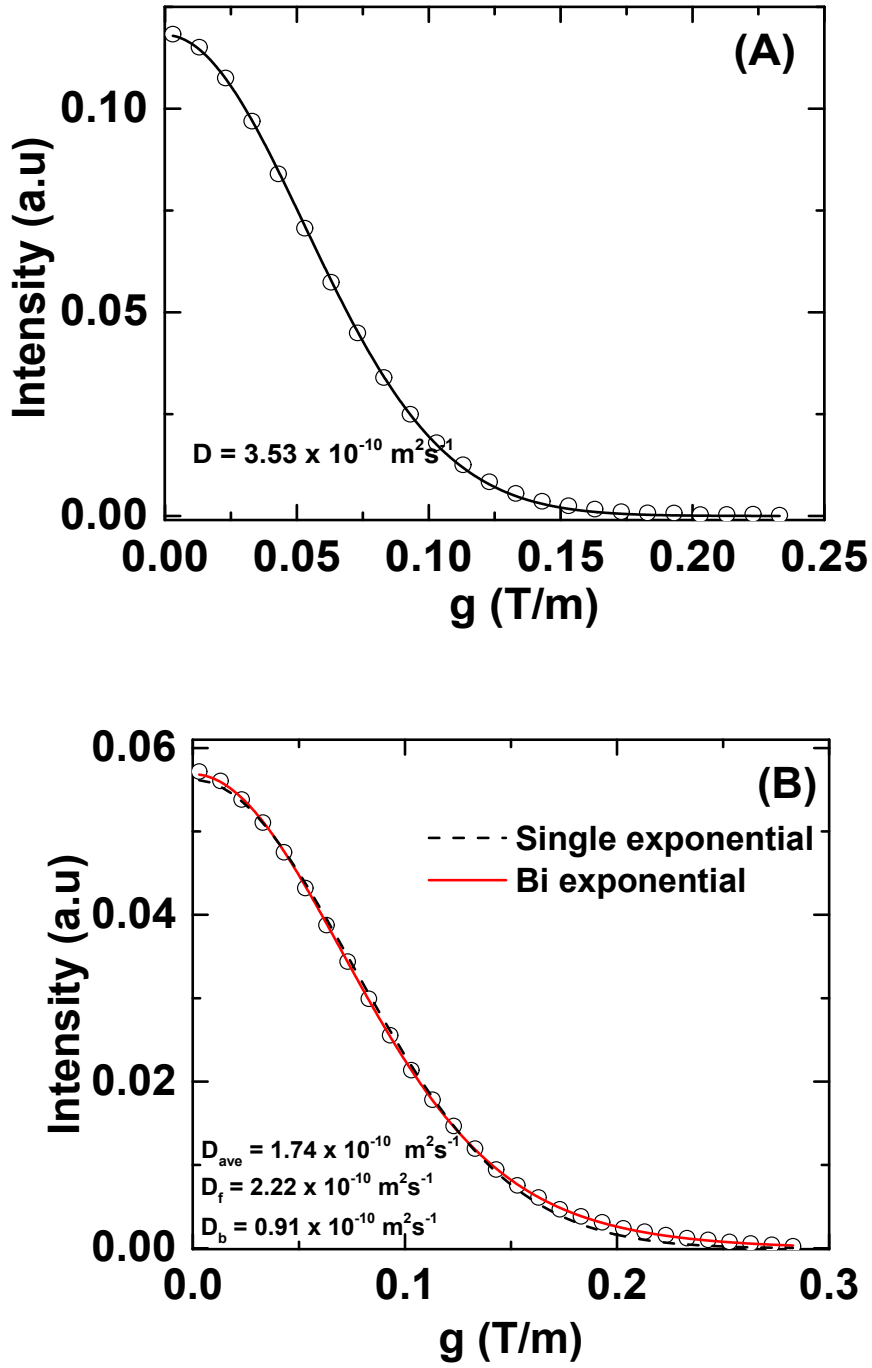

Figure S5 Pulse field gradient NMR signal attenuation plots for (A) $(mPEG_4)_2SO_3Na$ and (B) $(mPEG_{23})_2SO_3Na$ at 298K; the solid line represents the best Arrhenius fit (single exponential) of the experimental data, and the dotted line represents bi-exponential fit ($I = ae^{-kD_1} + be^{-kD_2}$) for the $(mPEG_{23})_2SO_3Na$.

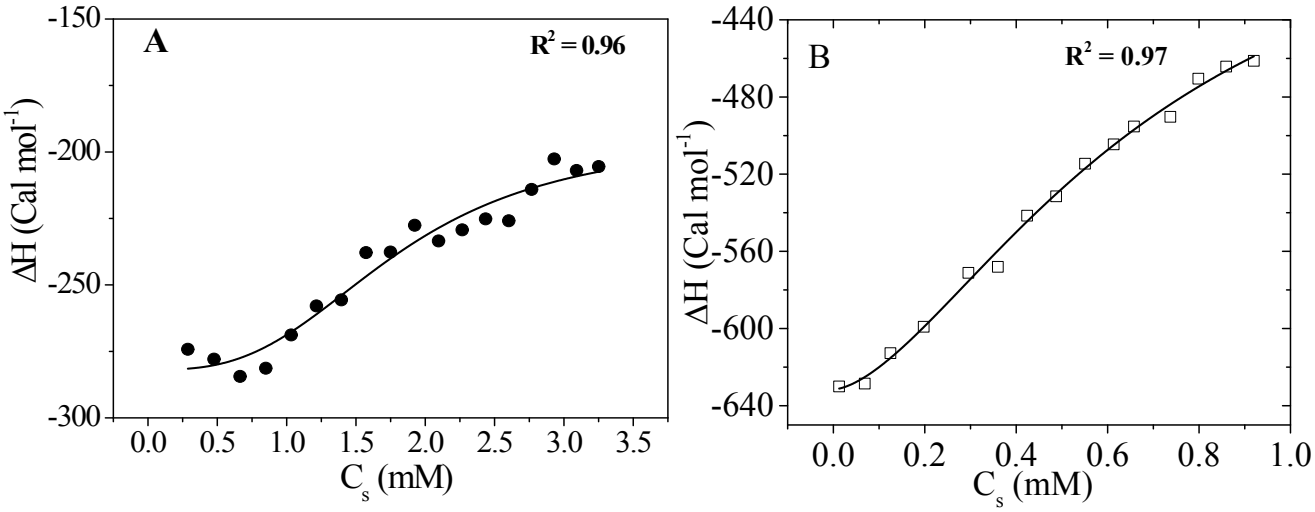

Figure S6 Plots of variation of change in enthalpy (ΔH) versus C_s at 25 °C of (A) $(mPEG_4)_2SO_3Na$ and (B) $(mPEG_{23})_2SO_3Na$.

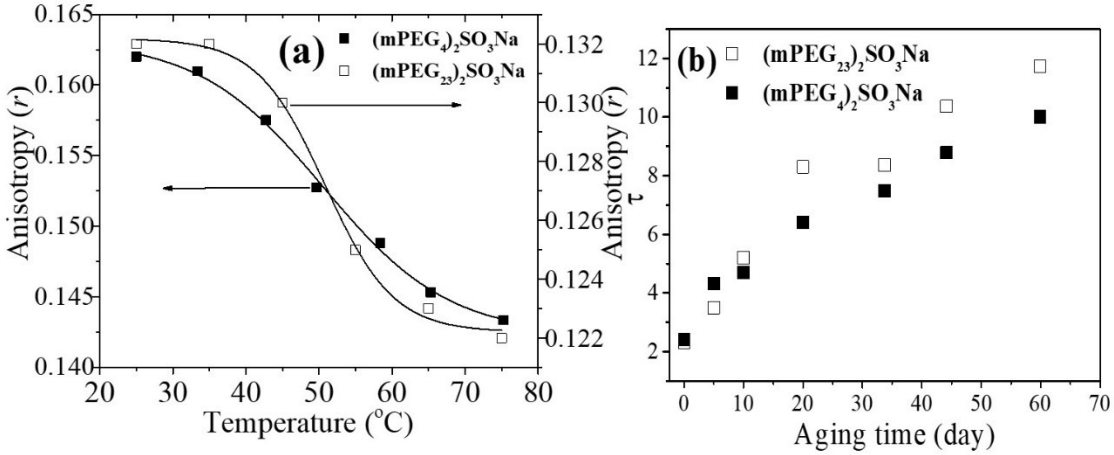

Figure S7 (a) Variation of *r* value of DPH in the presence of $(mPEG_4)_2SO_3Na$ (5 mM) and $(mPEG_{23})_2SO_3Na$ (5 mM) with temperature (°C), and (b) plots of τ versus aging time at 25 °C.

Table S2 Variable-temperature T_1 and T_2 data of $(mPEG_4)_2SO_3Na$.

Temp ℃	T_{2a} (s)	Error (±)	T_{1a} (s)	Error (±)	T_{2b} (s)	Error (±)	T_{1b} (s)	Error (±)	T_{2g} (s)	Error (±)	T_{1g} (s)	Error (±)
25	2.519	0.0692	3.1282	0.0240	0.9054	0.0049	0.9708	0.0039	0.6255	0.0126	0.7473	0.0024
30	2.6103	0.0323	3.6526	0.0178	0.9910	0.0090	1.1237	0.0045	0.6806	0.0104	0.812	0.0029
35	3.0252	0.0307	3.9407	0.0316	1.1269	0.01181	1.2299	0.0047	0.7677	0.0131	0.8830	0.0027
40	3.5871	0.0251	4.4910	0.0275	1.2985	0.0090	1.3829	0.0063	0.8099	0.0128	0.9623	0.0042
45	4.1501	0.0141	5.0752	0.0205	1.4643	0.0080	1.5430	0.0053	0.9138	0.0083	1.043	0.0045
50	4.3052	0.0170	6.7114	0.0862	1.6211	0.0086	1.8111	0.0078	0.9857	0.0120	1.1434	0.0036

Table S3 Variable-temperature T_1 and T_2 data of $(mPEG_{23})_2SO_3Na$.

Temp ℃	T_{2a} (s)	Error (±)	T_{1a} (s)	Error (±)	T_{2b} (s)	Error (±)	T_{1b} (s)	Error (±)	T_{2g} (s)	Error (±)	T_{1g} (s)	Error (±)
25	2.4573	0.0525	2.9958	0.0262	0.6040	0.0037	0.7371	0.0012	0.519	0.0263	0.663	0.0031
30	2.5493	0.0431	3.4152	0.0295	0.6904	0.0034	0.8213	0.0017	0.5269	0.0155	0.7093	0.0038
35	3.2611	0.0320	3.8117	0.0299	0.7862	0.0054	0.9084	0.0019	0.5916	0.0208	0.7655	0.0043
40	3.5120	0.0444	4.3131	0.0267	0.8695	0.0048	1.0016	0.0014	0.6613	0.0175	0.8793	0.021
45	3.8913	0.0654	4.6339	0.0415	0.9870	0.0099	1.1399	0.0040	0.7063	0.0463	0.8998	0.0056
50	4.2656	0.1057	5.9383	0.1774	1.1184	0.0137	1.6605	0.0267	0.7733	0.0450	1.0425	0.0072

References

[1] R. Ghosh, and J. Dey, *J. Colloid Interface Sci.* 2015, **451**, 53–62.

[2] R. Ghosh, and J. Dey, *J. Langmuir* 2017, **33**, 543–552.

[3] R. Ghosh, and J. Dey, *Langmuir* 2014, **30**, 13516–13524.

[4] R. K. Harris, Nuclear Magnetic Resonance Spectroscopy, Longman, London, 1986.

[5] D. H. Wu, A. D. Chen, and C. S. Johnson, *J. Magn. Reson., Ser. A* 1995, **115**, 260-264.

[6] B. V. N. Phani Kumar, U. S. Priyadharsini, G. K. S. Prameela, and A. B. Mandal, *J. Colloid Interface Sci.* 2011, **360**, 154-162.

[7] E. O. Stejskal, and J. E. Tanner, *J. Chem. Phys.*1965, **42**, 288-292.

[8] J. R. Lakowicz, Principles of Fluorescence Spectroscopy, Plenum Press, New York, 1983, p. 132.

[9] P. Debye, Polar Molecules, Dover, New York, 1929.

[10] S. Roy, S. Mohanty, and J. Dey, *Chem. Phys. Lett*. 2005, **414**, 23-27.

[11] M. Shinitzky, and Y. Barenholz, *J. Biol. Chem.* 1974, **249**, 2652–2657.

[12] R. E. Verrall, S. Milioto, and R. Zana, *J. Phys. Chem*. 1988, **92**, 3939−3943.

[13] P. R. Majhi, and S. P. Moulik, *Langmuir* 1998, **14**, 3986−3990.